

Evaluation of diffusion length and surface recombination velocity in semiconductor devices by the method of moments

A. Cavallini, B. Fraboni, and D. Cavalcoli

Citation: *Journal of Applied Physics* **71**, 5964 (1992); doi: 10.1063/1.350447

View online: <http://dx.doi.org/10.1063/1.350447>

View Table of Contents: <http://scitation.aip.org/content/aip/journal/jap/71/12?ver=pdfcov>

Published by the [AIP Publishing](#)

Articles you may be interested in

[Nanoscopic measurements of surface recombination velocity and diffusion length in a semiconductor quantum well](#)

Appl. Phys. Lett. **81**, 346 (2002); 10.1063/1.1492307

[Evaluation of the minority carrier diffusion length and edge surface-recombination velocity in GaAs p/n solar cells](#)

J. Appl. Phys. **72**, 2919 (1992); 10.1063/1.351494

[A contactless method for determination of carrier lifetime, surface recombination velocity, and diffusion constant in semiconductors](#)


J. Appl. Phys. **63**, 1977 (1988); 10.1063/1.341097

[Evaluation of diffusion length and surface-recombination velocity from a planar-collector-geometry electron-beam-induced current scan](#)

J. Appl. Phys. **57**, 2077 (1985); 10.1063/1.334400

[Evaluation of diffusion lengths and surface recombination velocities from electron beam induced current scans](#)

Appl. Phys. Lett. **43**, 120 (1983); 10.1063/1.94139



SHIMADZU

Excellence in Science

Powerful, Multi-functional UV-Vis-NIR and FTIR Spectrophotometers

Providing the utmost in sensitivity, accuracy and resolution for applications in materials characterization and nano research

- Photovoltaics
- Polymers
- Thin films
- Paints

- Ceramics
- DNA film structures
- Coatings
- Packaging materials



[Click here to learn more](#)

Evaluation of diffusion length and surface recombination velocity in semiconductor devices by the method of moments

A. Cavallini, B. Fraboni, and D. Cavalcoli

Department of Physics, University of Bologna, Via Irnerio 46, I-40126 Bologna, Italy

(Received 4 November 1991; accepted for publication 26 February 1992)

The diffusion length and surface recombination velocity of the minority carriers are determined from electron beam induced current (EBIC) profiles on a semiconductor containing a barrier perpendicular to the scanned surface. The evaluation of both the parameters has been obtained by the procedure called "of the first moments," due to Donolato [C. Donolato, Appl. Phys. Lett. **43**, 120 (1983)], which is based on the calculation of the first moment about the origin of two induced current profiles. This analysis, based on an exact integral property of the EBIC scans, allows evaluation of the diffusion length and the surface recombination without fitting the experimental profiles. In addition, it is easy to handle and can also be readily applied to real devices.

I. INTRODUCTION

A number of scanning electron microscopy methods based on the measurement of the electron beam induced current (EBIC) profiles have been established for the assessment of semiconducting materials.¹ As a matter of fact, EBIC is a convenient technique for the determination of the minority carrier diffusion length L and, occasionally, of the surface recombination velocity v_s , which characterizes semiconducting bulk materials and their dependence on the growth conditions, as well as devices and the effects of their manufacture.

A widely used method for the determination of L and v_s refers to p - n junctions or Schottky barriers viewed edge-on. In this configuration, called "normal collector geometry," the electron beam scans the semiconductor perpendicular to the junction (Fig. 1). The diffusion length L of minority carriers is derived from the variation of the electron beam induced current $I(x)$ with the junction beam distance x .

With the assumption of zero electric field outside the junction space charge region, the transport of beam-generated excess carriers can be considered purely diffusive. Under this condition and if the surface recombination velocity v_s is equal to zero, the induced current decreases with increasing distance from the collecting region as $\exp(-x/L)$.

When the surface recombination cannot be neglected, the diagram of $\log(I)$ as a function of x is no longer linear, but appears concave upward near the junction, being steeper and steeper with increasing v_s . General theoretical expressions for the induced current profile which incorporate the effects of the surface recombination velocity have been formulated, either referring back to the solution of the diffusion problem given by van Roosbroeck² for a point source of minority carriers at a depth z , or considering an extended generation.³⁻⁸ However, only in limiting cases ($v_s \rightarrow 0$, $v_s \rightarrow \infty$) is an analytical expression of $I(x,z)$ found which has an exact solution, whereas for arbitrary v_s it requires numerical computations. Therefore, if we don't resort to asymptotic solutions, the problem of extracting

accurate values for L and v_s can only be solved by fitting the experimental scans to the theory. Even though this has been done,¹ it implies unwieldy numerical calculations.

Instead of the complicated expression of the current profile in terms of integrals of modified Bessel functions,⁴ Donolato developed a simpler expression for $I(x,z)$ by the Fourier transform treatment⁸ and suggested an alternative way⁹ to evaluate diffusion length and surface recombination velocity through the calculation of first order moments of $I(x,z)$ about the x coordinate origin.

This paper deals with the application of this theoretical procedure which, to the knowledge of the authors, has never been utilized before. Indeed, this method has been applied as an example of data from literature by Donolato himself, but nobody has applied it to experimental data acquired just for this kind of elaboration. After a short outline of the method of first order moments, this paper presents the results obtained by applying it to p - n junctions and to p^+ - p - n diodes. The consistency of the method is assessed by comparing its results with those obtained by the procedure proposed by Davidson and Dimitriadis¹⁰ for the correction of diffusion length measurements for surface recombination. The main conclusions are summed up in Sec. V.

II. THEORETICAL APPROACH

The general theoretical expression for the EBIC signal derived from the steady-state diffusion equation for minority carriers in a neutral region, for instance in an n -type material, is:¹

$$\nabla^2 p(\mathbf{r}) - \frac{1}{L^2} p(\mathbf{r}) = -\frac{1}{D} g(\mathbf{r}), \quad (1)$$

where $p(\mathbf{r})$ is the excess hole density at the position $\mathbf{r} = (x,y,z)$, D and L their diffusion coefficient and diffusion length, respectively, and $g(\mathbf{r})$ the generation rate of electron-hole pairs per unit volume.

Donolato⁸ assessed that the transport of beam generated minority carriers is governed by a two-dimensional

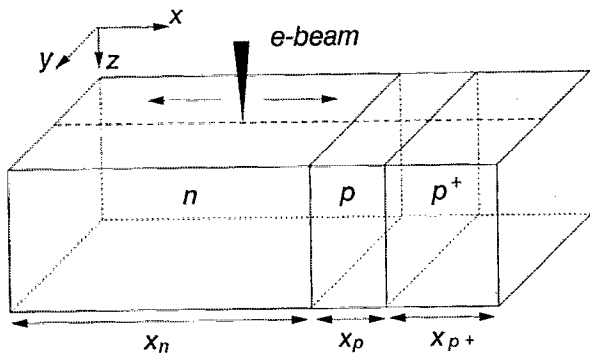


FIG. 1. Schematic view of the experimental configuration.

equation because of the translational invariance along the y axis of the normal collector geometry (Fig. 1). Therefore, expression (1) reduces to

$$\nabla^2 q(x, z) - \frac{1}{L^2} q(x, z) = -\frac{1}{D} h(x, z), \quad (2)$$

where q and h correspond, in the two-dimensional treatment, to p and g , respectively. This equation has to be solved with the boundary conditions

$$\begin{aligned} \text{(i)} \quad q &= 0 \quad \text{at } x=0 \\ \text{(ii)} \quad \frac{\partial q}{\partial z} &= sq \quad \text{at } z=0. \end{aligned} \quad (3)$$

Condition (i) expresses the fact that minority carriers are quickly swept away by the built-in electric field of the junction, and it only holds in the low level injection regime; condition (ii) introduces the phenomenological surface recombination velocity $s = v_s/D$. In addition to the above conditions, Eq. (2) is valid only if the material is uniformly doped and if L is small compared to the lateral dimensions of the specimen.^{11,12}

As a consequence of the simplification of the diffusion equation, the expression for the charge-collection probability found in Ref. 9, which only contains elementary functions, is:

$$Q(x, z) = \frac{2}{\pi} \int_0^\infty \Psi(k, z) \sin(kx) dk, \quad (4)$$

where $x > 0$, $z \geq 0$, and

$$\begin{aligned} \Psi(k, z) &= \frac{k}{k^2 + \lambda^2} \left\{ 1 - \frac{s}{(k^2 + \lambda^2)^{1/2} + s} \right. \\ &\quad \left. \times \exp[-(k^2 + \lambda^2)^{1/2} z] \right\}. \end{aligned} \quad (5)$$

In Eq. (5), $\lambda = 1/L$.

It is noteworthy that $Q(x, z)$ not only represents the fraction of injected minority carriers at (x, z) that flows into the junction, i.e., the carrier collection probability at the point (x, z) , but also gives the current profile $I(x, z)$ normalized to $I(0, z)$, due to a point source at z [i.e., for $h(x, z) = \delta(x - x') \cdot \delta(z - z')$, with δ Dirac function].

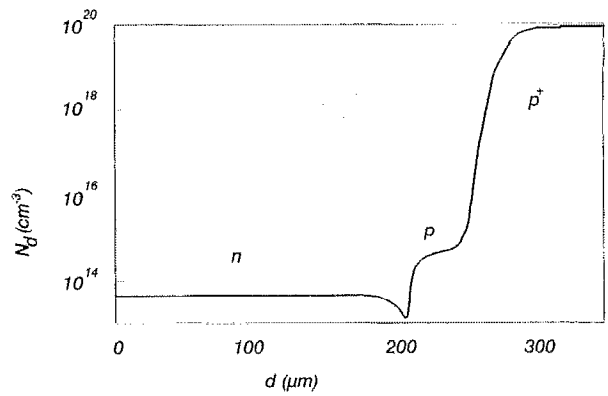


FIG. 2. Doping concentration profile of the p^+ - p - n structures analyzed, obtained from spreading resistance measurements.

Starting from this expression of the charge collection probability, the assessment of L and s can be made by the “method of moments.”

In what follows, “moment” means, as in statistics, the first moment about the origin of a probability distribution $Q(x, z)$, namely:

$$m(z) = \int_0^\infty x Q(x, z) dx. \quad (6)$$

By using in Eq. (4) the moment theorem for Fourier transforms,⁹ one gets:

$$m(z) = L^2 \{ 1 - [sL / (1 + sL)] \exp(-z/L) \}. \quad (7)$$

Equation (7) also holds for an extended generation, if z is interpreted as the center of gravity of the source function, which for the Everhart and Hoff generation¹³ is given by $z \cong 0.41R$ (R is the primary electron range).

EBIC profiles obtained with known generation depths z_1 and z_2 yield a two-equation system where L and s are the unknown quantities. Their values are easily found by reducing the system to an equation that can be numerically solved.

From what is said above, it is evident that the “moments” procedure is a powerful tool for independently deriving both L and s , and therefore v_s , overtaking the laboriousness of the calculations involved in theoretical curve-fitting procedures.

III. EXPERIMENTAL DETAILS AND DATA ANALYSIS

Planar junctions perpendicular to the beam scanned surface have been examined. Two kinds of devices with this configuration have been studied: p - n diodes and p^+ - p - n diodes. The former structure has been obtained by diffusion of B in a P doped bulk material, whereas the latter has been obtained by B and Al diffusion, that gives rise to the junction net doping profile shown in Fig. 2, which reports the impurity concentration curve obtained from spreading resistance measurements. Both kinds of devices had the same background doping level ($N_D - N_A = 6 \times 10^{13} \text{ cm}^{-3}$).

The EBIC measurements have been performed in a Philips 515 scanning electron microscope (SEM), connected with a computerized data acquisition system so as

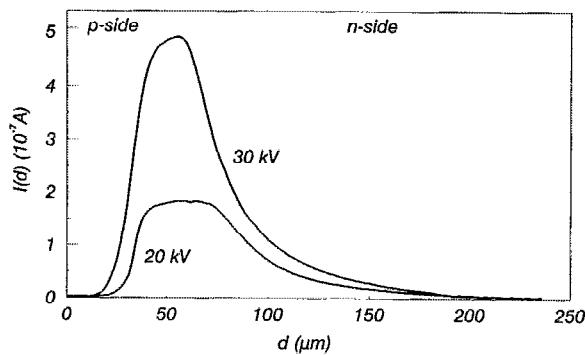


FIG. 3. Electron beam induced current I vs beam position d relative to p - n junction line scans of the same region at two beam energies.

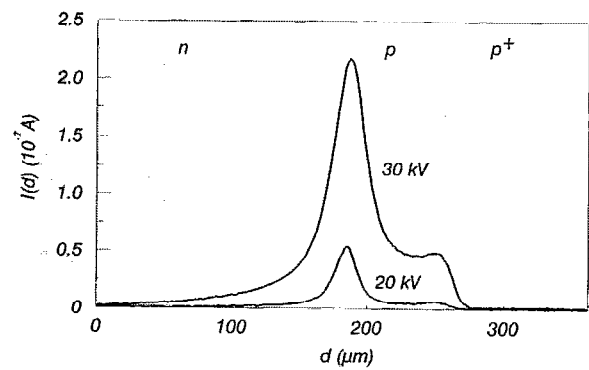


FIG. 5. EBIC profiles relative to p^+ - p - n structure at different beam energies.

to obtain good resolution and accuracy. In order to change the beam penetration depth z , the beam energy E_b has been varied from 10 to 30 keV. Figure 3 shows two EBIC profiles relative to p - n junction scan lines at two beam voltages E_b .

Since the moments method requires the specification of the origin of the x coordinate, i.e., of the depletion layer edge, this point has been located at the inflection point of the electron beam induced current profile. Even though it is based on qualitative arguments only, this choice has been made since the theoretical current curves where local charge neutrality may be assumed^{7,9} are concave upward.

The normalized EBIC profiles $i(x,z) = I(x,z)/I(0,z)$ relative to one side of the junction, e.g., the p side of the p - n junction,

$$i(x_p, z) = I(x_p, z)/I(0, z) \quad \text{for } z = z_1, z_2 \quad (8)$$

have been calculated and the typical domed plots $x_p i(x_p, z)$ vs x_p have been drawn (Fig. 4).

The first order moments

$$m(z) = \int_0^\infty x_p i(x_p, z) dx \quad (9)$$

for $z = z_1, z_2$ have been numerically evaluated and L and v_s determined by means of Eq. (7). The same steps have been

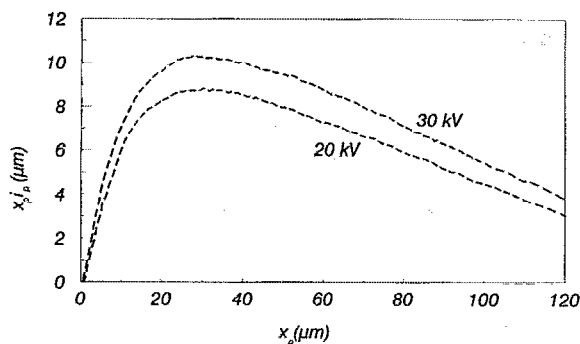


FIG. 4. Plot of the function $x_i i(x)$ vs the distance from the edge of the diffusion region at two beam energies.

followed for the EBIC line scan portions referring to the n side.

The method of moments has been applied to p^+ - p - n structures as well, where an additional maximum of the EBIC profile occurs at the p^+ - p junction (Fig. 5) because of the distribution of the electrostatic potential ψ , which reflects the doping profile.

The field associated with the doping gradient at the high-low concentration region of the diode gives rise to the "bulk electron voltaic effect" (bulk EVE),¹ thus generating a charge collection signal from the electromotive forces that exist in the specimen at the junction. In this case the method has been applied to each of the three portions of the EBIC scans which refer to uniform doping conditions for extracting the corresponding L and v_s .

The evaluation of m is straightforward for the end regions of the device, but implies more care in the intermediate one since its electron beam induced current tail is partially hidden by the overlapping of the high-low junction signal. For evaluating the moment from the available values in the p region, it is therefore necessary to resort to a fitting procedure to make up for the lack of experimental data of the tail. First of all the location $x_{p,0}$ of the edge of the p - n junction has been determined, then the concave part of the curve has been analyzed to identify the coordinate x_e from which the experimental trend is fitted with an exponential. Then, the moment referring to the p side has been evaluated numerically for $x_{p,0} \leq x < x_e$ and analytically, according to the exponential behavior, over the interval (x_e, ∞) .

TABLE I. Results obtained from the application of the method of moments to p - n and p^+ - p - n diodes.

Structure	Region	L (μm)	sL	v_s (10^5 cm/s)
p - n	p	5.0 ± 0.3	25 ± 3	8.0 ± 0.6
	n	97 ± 4	19 ± 1	0.30 ± 0.1
p^+ - p - n	p^+	2.0 ± 0.1	3.0 ± 0.6	2.0 ± 0.3
	p	15.0 ± 0.6	56 ± 9	6.0 ± 0.8
	n	139 ± 5	37 ± 5	0.03 ± 0.01

IV. RESULTS AND DISCUSSION

The results obtained are summed up in Table I. The errors indicated result from the indetermination associated with the numerical evaluation of the area bounded by the $i(x,z)$ curves and the x axis, due mainly to the noise on the tails. In fact, contrary to what is expected, the error due to the evaluation of the EBIC profile origin $x=0$ scarcely affects the value of the moments and, hence, of the diffusion length and of the surface recombination velocity. This happens, in our opinion, because the determination of the depletion layer edge has been performed on data that (i) refer to a high charge collection probability, i.e., to a high short circuit current signal, and (ii) have been acquired with spatial resolution controlled via computer. On the contrary, the statistical weight of the tails on the overall error is heavier, since the induced current varies over many orders of magnitude with the distance from the junction and it becomes almost comparable to the noise itself when $x \rightarrow \infty$.

Due to the importance of the requirements of the low-level injection conditions for an appropriate application of the theoretical approach in the present cases, we assessed the used injection levels in terms of the beam current and voltage, on the basis of the Berz and Kuiken treatment.⁴ Since all the surface recombination velocity values obtained are large (see Table I), only the case when $v_s = \infty$ has been taken into consideration. In this case, in regard to the example in the n region, the injected hole density Δp_b is given by

$$\Delta p_b = \frac{5}{2\pi} \frac{G\tau_1}{L_1^3} \frac{h_0}{L_1} \quad (10)$$

with τ_1 and L_1 lifetime and diffusion length, respectively, at low injection and

$$G = 1.6 \times 10^{18} I_b E_b$$

$$h_0 = 3.84 \times 10^{-12} E_b^{1.75}, \quad (11)$$

where I_b is the beam current in A, E_b is the beam voltage in V, and h_0 in cm. In the investigated cases the low injection conditions resulted were everywhere fulfilled, since the beam current used was $I_b < 5 \times 10^{-9}$ A and the beam energy < 30 keV.

As regards the p^+-p-n diodes, particular attention has to be paid to studying these structures in order to verify how the distance between the $p-n$ junction and the high-low barrier affects the induced current. As a matter of fact, effects of the distribution of electric fields and carrier lifetimes on EBIC profiles have to be taken into account,^{14,15} since the conventional models only consider a limited extension of the field region or, in other words, electric field equal to zero throughout the crystal.

Thus, EBIC line scans for a set of different external generation rates, i.e., beam currents, have been generated to check if the distance from the high-low junction to the $p-n$ junction exceeds the actual diffusion length. Since a characteristic feature of extended field regions is a strong dependence of the EBIC profile shape on the beam current,¹⁵ this analysis would have shown the presence of pos-

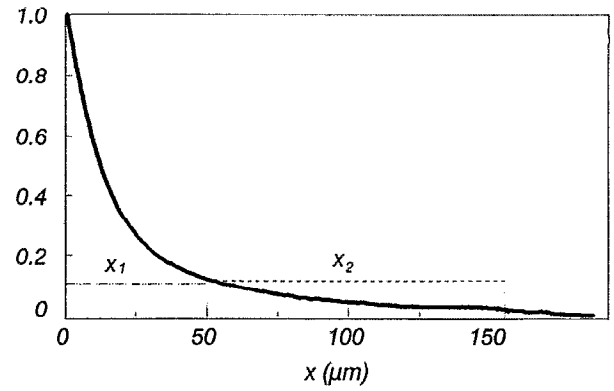


FIG. 6. Normalized collected current profiles $i(x,z)$ vs distance x from the edge of the diffusion region, for the n side of a $p-n$ diode.

sible electric fields far outside the conventional field regions, either due to the $p-n$ junction or to the p^+-p reflecting barrier. As no effect on the curve shape has been observed, we assumed no electric field at the excitation site inside the p region.

The assumption of neglecting the back contact effect^{11,12} due to the sample surface or to a reflecting barrier holds since in each explored region of length d_0 , is $2L < d_0$.¹⁰ While analyzing these real devices, it is important to show that the p^+ end region of the diodes is in a degenerate condition. However, this is not a limiting condition in the analysis of electron beam induced current profiles, since the conventional EBIC approach assumes low level injection. Von Roos¹⁶ demonstrated that in this regime and if we are dealing with a wide band gap semiconductor such as silicon, the minority carrier distribution is nondegenerate even if the majority carrier distribution is degenerate. Therefore, from the assumptions of low-level injection and of pure carrier diffusion, i.e., local charge neutrality, it follows that the Shockley-Read-Hall theory can be extended to degenerate semiconductors and the recombination-generation current derivation is basically identical to the one formulated for nondegenerate semiconductors.

The above evaluation of the diffusion length L by the method of first moments takes into account the surface recombination velocity v_s . A check of the consistency of the present results has been carried out by means of the procedure of Davidson and Dimitriadis,¹⁰ deduced from the theoretical EBIC characteristics calculated from the analysis of Berz and Kuiken.⁴

A rough estimate L_{exp} of the diffusion length can be achieved from the slope of the linear part of $\ln[i(x)]$ of the experimental EBIC scans. The value so obtained does not take into consideration the surface recombination velocity effect on the EBIC profile and, thus, results $L_{exp} < L$.^{4,9,12} From the theoretical treatment of the continuity equation for extracting the true diffusion length L , Davidson and Dimitriadis stressed how the ratio x_1/x_2 (Fig. 6) strongly depends on L/L_{exp} , since the larger the v_s , the steeper is the characteristic of the theoretical EBIC versus junction beam distance. As reported in Fig. 6, x_1 is the beam coordinate

TABLE II. Comparison between diffusion length values obtained with the method of moments, (Ref. 9) L , and that reported in Ref. 10, L^* .

L (μm)	L_{exp} (μm)	x_1/x_2	L^*/L_{exp}	L^* (μm)
63 ± 2	48.0 ± 0.3	0.63 ± 0.01	0.77 ± 0.02	62 ± 2

corresponding to a decrease of one order of magnitude in the induced current from its maximum value, and x_2 is the distance from x_1 to the position corresponding to a further current decrease of one decade. Thus we have followed the procedure reported below for testing the method of moments: (a) L_{exp} has been evaluated from the behavior of the EBIC profiles for $x \rightarrow \infty$, (b) the ratio x_1/x_2 has been calculated, and (c) the corresponding theoretical value L/L_{exp} from Ref. 10 has been found and the value L obtained by it times L_{exp} has been compared to the diffusion length L deduced by the moments method.

As shown in the example reported in Table II, the agreement between the theoretical calculations from Ref. 10 and the results of the present work is very good.

V. CONCLUSIONS

This paper has taken into account that the determination of minority carrier diffusion length L and surface recombination velocity v_s by means of the method of moments with a SEM operating in the normal collector configuration is a very useful tool for analyzing devices. The method is based on the calculation of first order moments about the origin of EBIC profiles and offers a convenient determination of the parameters L and s , and from this of v_s . It implies the determination of the location of the depletion layer edge, that at first sight would seem a disadvantage in respect to other procedures.^{17,18} However, the error in L derived from the choice of the x axis zero is confined to a few percent since the procedure is not based on the asymptotic behavior of the electron beam induced current $i(x)$ (which implies a mean correction factor $L_{\text{exp}} \approx 0.7L^4$), but on the measurement of its first order moment m about the origin that is on an exact integral property of the EBIC line scans. Indeed, the evaluation of m , given by the numerical calculation of the area subtended by the curve $xi(x)$, is sensitive to both the location of the origin of the x coordinate (which is very low) and the noise on the $i(x)$ tail.

The following remarks can hence be made:

(i) With computer controlled data acquisition the uncertainty Δx in the position of the electrical junction edge reduces to a very low value, so as not to considerably affect L , as the error associated with it remains approximately constant ($\leq 3\%$), and to scarcely affect v_s at all.

(ii) The presence of noise on the profile tail has a greater influence on the determination of L and v_s . But while L is not particularly influenced by it and the associated error remains limited, v_s is more closely related to the shape of the tail. However, since the whole calculation is mainly based on the large area bounded by the domed

portion of the first moment curve, the weight of the integral close to the origin is greater than on the tail, and this results in a substantial reduction of the errors associated with the measurements of L and v_s , if compared to methods that rely on the asymptotic behavior of the tails. The errors given in Table I result from the standard deviation of the parameters of Eq. (7).

Besides, no *a priori* assumptions on v_s are needed for evaluating L , and the values of L and v_s are obtained from the numerical solution of systems of algebraic equations rather than from a two-parameter fitting of experimental curves.

A check of the consistency of the results obtained by the moments method by comparing them with those derived through the procedure of Davidson and Dimitriadis is very satisfactory. In fact, both methods start from the same theoretical considerations, but while the former determines L and v_s by calculating the area subtended by $xi(x)$, the latter reaches the same goal by considering the steepness dependence of $I(x)$ on L and v_s .

Finally, the method of moments is reliable and straightforward in the assessment of the L and v_s values not only for p - n junctions but also for more complicated structures, and sufficiently rapid to be practical.

ACKNOWLEDGMENTS

The authors are particularly indebted to A. Castaldini for his numerous and fruitful comments throughout the course of the work and gratefully acknowledge Dr. C. Donolato for helpful discussion. This work has been supported by MPI grants of the Italian Ministry of Education.

¹ For a wide range of literature, see D. B. Holt and D. C. Joy, *SEM Microcharacterization of Semiconductors* (Academic, London, 1989).

² W. van Roosbroeck, *J. Appl. Phys.* **26**, 380 (1955).

³ J. F. Bresse, in *Proceedings of the 5th Ann. SEM Symposium IITRI*, edited by O. Johary and I. Corvin (IIT Research Institute, Chicago, 1972), pp. 105-112.

⁴ F. Berz and H. K. Kuiken, *Solid State Electron.* **19**, 437 (1976).

⁵ C. van Opdorp, *Philips Res. Rept.* **32**, 192 (1977).

⁶ T. Fuyuki, H. Matsunami, and T. Tanaka, *J. Phys. D: Appl. Phys.* **13**, 1093 (1980); *ibid.* **13**, 1503 (1980).

⁷ G. Oelgart, J. Fiddicke, and R. Reulke, *Phys. Status Solidi A* **66**, 283 (1981).

⁸ C. Donolato, *Solid-State Electron.* **25**, 1077 (1982).

⁹ C. Donolato, *Appl. Phys. Lett.* **43**, 120 (1983).

¹⁰ S. M. Davidson and C. A. Dimitriadis, *J. Microsc.* **118**, 275 (1980).

¹¹ O. von Roos, *Solid-State Electron.* **21**, 1063 (1978); **21**, 1069 (1978).

¹² T. Fuyuki and H. Matsunami, *Jpn. J. Appl. Phys.* **20**, 745 (1981).

¹³ T. E. Everhart and P. H. Hoff, *J. Appl. Phys.* **42**, 5837 (1971).

¹⁴ S. M. Davidson, R. M. Innes, and S. M. Lindsay, *Solid-State Electron.* **25**, 261 (1982).

¹⁵ H. W. Marten and O. Hildebrand, *Scanning Electron Microsc.* **III**, 1197 (1983).

¹⁶ O. von Roos, *J. Appl. Phys.* **48**, 5389 (1977); *Solid-State Electron.* **21**, 633 (1978).

¹⁷ C. Donolato, *Solid-State Electron.* **28**, 1143 (1985).

¹⁸ D. Cavalcoli, A. Cavallini, and A. Castaldini, *J. Appl. Phys.* **70**, 2163 (1991).